Available online at www.sciencedirect.com
ScienceDirect
Journal of Organometallic Chemistry 692 (2007) 768–773
Journal of Organometallic Chemistry
www.elsevier.com/locate/jorganchem

Reactivity of the heteronuclear cluster $RuOs_3(\mu\text{-}H)_2(CO)_{13}$ with indene

Yong Leng Kelvin Tan, Weng Kee Leong *

Department of Chemistry, National University of Singapore, Kent Ridge, Singapore 119260, Singapore

Received 18 September 2006; received in revised form 6 October 2006; accepted 6 October 2006
Available online 13 October 2006

Abstract

The heteronuclear cluster $RuOs_3(\mu\text{-}H)_2(CO)_{13}$ (**1**) reacts with indene under thermal activation to afford the novel clusters $RuOs_3(\mu\text{-}H)(CO)_9(\mu\text{-}CO)_2(\eta^5\text{-}C_9H_7)$ (**3**), $RuOs_3(\mu\text{-}H)(CO)_9(\mu_3,\eta^5\text{:}\eta^2\text{:}\eta^2\text{-}C_9H_7)$ (**4**) and $Ru_2Os_3(\mu\text{-}H)(CO)_{11}(\mu_3,\eta^5\text{:}\eta^2\text{:}\eta^2\text{-}C_9H_7)$ (**5**), the latter two possessing indenyl ligands in the $\mu_3,\eta^5\text{:}\eta^2\text{:}\eta^2$ bonding mode. Cluster **5** exists as a mixture of two isomers. The inter-relationship among the clusters has also been investigated.

Keywords: Heterometallic clusters; Ruthenium; Osmium; Isomers; Indene

1. Introduction

Studies of polycyclic aromatics such as indene enable a direct comparison on the reactivity of multiple rings to be made, in addition to providing an insight into the interactions between π-systems and metal centers. Awareness of transition metal complexes incorporating the indenyl ligand as an important class of compounds for stoichiometric and catalytic asymmetric induction has increased over the last decade, with mono- and binuclear indenyl complexes being tested as potential Ziegler–Natta and Fischer–Tropsch catalysts [1]. This has revived interest in the reactivity of indene and indenyl derivatives with organometallic clusters. The reactivity of homonuclear carbonyl clusters with indene has been examined by several groups [2], although there has been comparatively few reports on their reactions with heteronuclear clusters [3]. We have recently initiated investigations into the chemistry of the group 8 heterotetranuclear cluster $RuOs_3(\mu\text{-}H)_2(CO)_{13}$ (**1**). It was envisaged that the ruthenium vertex in **1** would be more reactive than the osmium vertices. Hence, cluster **1** was expected to be less inclined to fragmentation of the cluster framework compared to homonuclear ruthenium clusters, and yet may react under relatively milder conditions than homonuclear osmium clusters. In this article, we present the results of our investigations into the reaction of **1** with indene.

2. Results and discussion

The reaction of **1** with indene at 120 °C afforded, upon TLC separation, besides unreacted **1** and $Os_3(\mu\text{-}H)_2(CO)_{10}$ (**2**) (probably a decomposition product of **1**), three novel clusters, viz., $RuOs_3(\mu\text{-}H)(CO)_9(\mu\text{-}CO)_2(\eta^5\text{-}C_9H_7)$ (**3**), $RuOs_3(\mu\text{-}H)(CO)_9(\mu_3,\eta^5\text{:}\eta^2\text{:}\eta^2\text{-}C_9H_7)$ (**4**) and $Ru_2Os_3(\mu\text{-}H)(CO)_{11}(\mu_3,\eta^5\text{:}\eta^2\text{:}\eta^2\text{-}C_9H_7)$ (**5**) in 35%, 9% and 24% yields (calculated with respect to consumed **1**), respectively. Shortening the reaction time afforded **3** and **5** but no **4**. All three novel clusters **3**–**5** have been studied by single crystal X-ray diffraction methods.

The ORTEP plot showing the molecular structure, together with selected bond parameters, for **3** is given in Fig. 1. Cluster **3** retains the tetrahedral metal framework of the parent cluster **1**, with the indenyl ligand capping the ruthenium atom. It is structurally similar to the reported cluster $RuOs_3(\mu\text{-}H)(CO)_9(\mu\text{-}CO)_2(\eta^5\text{-}C_5H_5)$, **3a**, which was synthesized from the reaction of $[Ru(C_5H_5)(MeCN)_3]^+$ with

* Corresponding author.
E-mail address: chmlwk@nus.edu.sg (W.K. Leong).

0022-328X/$ - see front matter © 2006 Elsevier B.V. All rights reserved.
doi:10.1016/j.jorganchem.2006.10.010

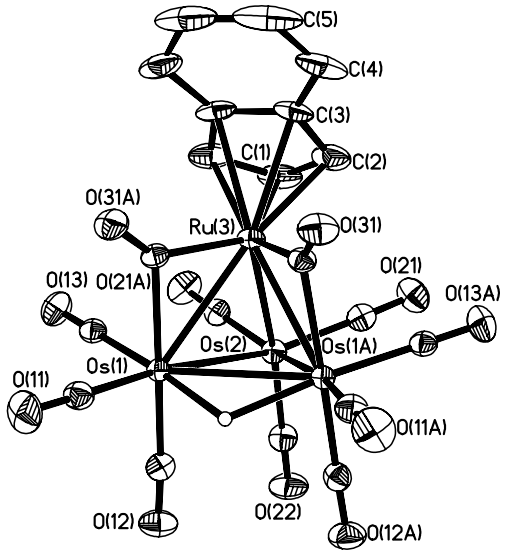

Fig. 1. ORTEP diagram (50% probability thermal ellipsoids, organic hydrogens omitted) and selected bond lengths (Å) and angles (deg) for **3**. Os(1)Os(1A) = 2.9489(3); Os(1)Os(2) = 2.7839(3); Os(1)Ru(3) = 2.8175(5); Os(2)Ru(3) = 2.7635(5); Os(1)C(31A) = 2.224(5); Ru(3)C(31A) = 1.978(5); Ru(3)C(31)Os(1A) = 83.99(17).

$[Os_3H(CO)_{11}]^-$ [4]. The crystal structure of **3** possesses mirror symmetry; the crystallographic mirror plane passes through the Os(2)–Ru(3) vector and bisects the Os(1)–Os(1A) edge and the indenyl ligand. The distance from Ru(3) to the centroid of the five-membered ring is 1.929(6) Å. The indenyl ligand in **3** is oriented such that the six-membered ring is above the bridging carbonyl ligands, with the five-membered ring tilted at an angle of 33.6° with respect to the triosmium basal plane. This may be ascribed to steric interaction with the two bridging carbonyl ligands; the bridging carbonyl ligands enable the cluster to take up the additional electron density from the 'electron rich' $Ru(\eta^5\text{-}C_9H_7)$ fragment [5].

The ^{1}H NMR spectrum of **3** at ambient temperature shows a broad resonance at δ −21.66 ppm. On cooling to 183 K three resonances are prominent: a major singlet at δ −22.39 ppm and two minor singlets at δ −19.07 and −20.13 ppm, with relative intensity ratio of 57:1.0:1.0 (Fig. 2). These resonances may be ascribed to the presence of three isomers in solution. The major isomer may be assigned as that found in the solid state, while the other two presumably corresponded to the hydride bridging different metal–metal bonds. In accordance with previous observations for tetranuclear $RuOs_3$ clusters, where the hydrides bridging Ru–Os edges were found to resonate at a lower field relative to the hydrides bridging Os–Os edges [6], it may be assumed that the two minor isomers have the hydride bridging an Os–Ru edge but we could not be more definite about their structures.

The ORTEP plot showing the molecular structure, together with selected bond parameters, for **4** is given in Fig. 3. The metal framework of **4** consists of a closed tetrahedron with the indenyl group lying over one triangular face. As for **3**, it also has a total valence electron count of 60, consistent with the tetrahedral cluster framework. A hydride ligand bridges the Os(1)–Os(3) vector, but the longest metal-metal bonds involve Ru(4). All nine carbon

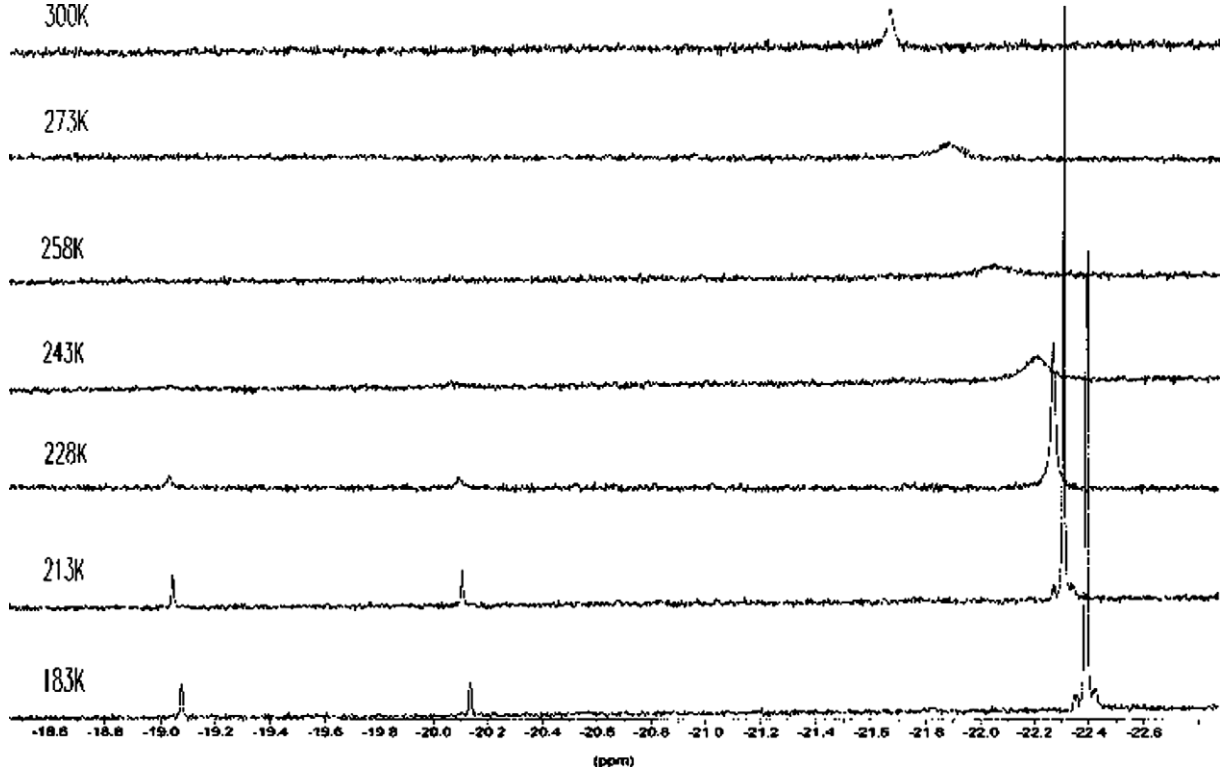

Fig. 2. Variable temperature ^{1}H NMR spectra (d_8-toluene) for **3**.

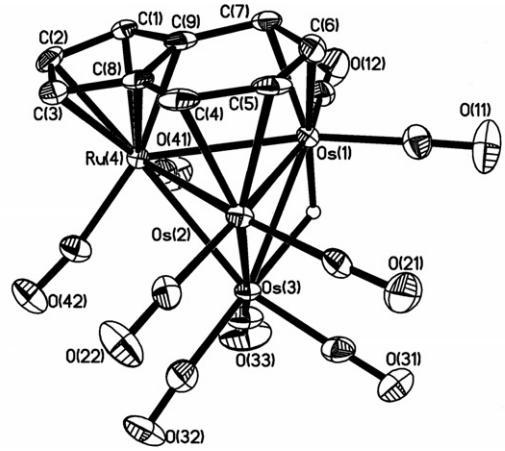

Fig. 3. ORTEP diagram (50% probability thermal ellipsoids, organic hydrogens omitted) and selected bond lengths (Å) for **4**. Os(1)Os(2) = 2.7909(7); Os(1)Os(3) = 2.8560(11); Os(1)Ru(4) = 2.9079(9); Os(2)Os(3) = 2.6670(8); Os(2)Ru(4) = 2.9749(12); Os(3)Ru(4) = 2.9543(9); Os(1)C(6) = 2.373(7); Os(1)C(7) = 2.197(7); Os(2)C(4) = 2.203(7); Os(2)C(5) = 2.250(6); Ru(4)C_5ring(centroid) = 1.893(7).

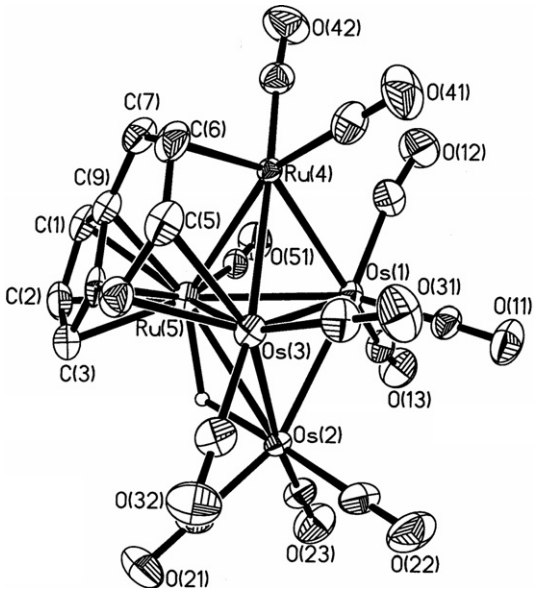

Fig. 4. ORTEP diagram (50% probability thermal ellipsoids, organic hydrogens omitted) and selected bond lengths (Å) for **5**. Os(1)Os(2) = 2.7283(5); Os(1)Os(3) = 2.7609(5); Os(1)Ru(4) = 2.6563(7); Os(1)Ru(5) = 2.8190(7); Os(2)Os(3) = 2.7723(5); Os(2)Ru(5) = 2.9241(7); Os(3)Ru(4) = 2.8203(7); Os(3)Ru(5) = 2.7989(7); Ru(4)Ru(5) = 2.8638(9); Os(3)C(4) = 2.216(9); Os(3)C(5) = 2.390(9); Ru(4)C(6) = 2.233(10); Ru(4)C(7) = 2.227(10); Ru(5)C_5 ring(centroid) = 1.869(9).

atoms of the indenyl moiety are coordinated to the Os(1)Os(2)Ru(4) trimetallic face, in what may be described as involving an η^5-cyclopentadienyl in addition to a η^2,η^2-diene. Thus the indenyl ligand acts formally as a nine-electron donor, reminiscent of the bonding situation found in the related homonuclear clusters $Os_4(\mu\text{-H})(CO)_9(\mu_3,\eta^5{:}\eta^2{:}\eta^2\text{-}C_{13}H_{15})$, $Os_4(\mu\text{-H})(CO)_9(\mu_3,\eta^5{:}\eta^2{:}\eta^2\text{-}C_{19}H_{17})$, $Ru_4(\mu\text{-H})(CO)_9(\mu_3,\eta^5{:}\eta^2{:}\eta^2\text{-}C_{19}H_{17})$ and $Ru_4(\mu\text{-H})(CO)_9(\mu_3,\eta^5{:}\eta^2{:}\eta^2\text{-}C_{22}H_{19})$ [2c,7]. Cluster **4** has also been characterized by infrared and proton NMR spectroscopies as well as FAB mass spectrometry.

The ORTEP plot showing the molecular structure, together with selected bond parameters, for **5** is given in Fig. 4. The metal core of **5** consists of a trigonal bipyramidal Ru_2Os_3 framework, with a valence electron count of 72, as predicted by the EAN rule [8]. The indenyl ligand is bonded in a similar fashion as found for **4**. It is noted that the ruthenium atom capped by the five-membered ring is found in an equatorial position in the metal core; there was no evidence for an isomer with the cyclopentadienyl ring of the indenyl ligand capping a metal atom at the axial site. This observation is consistent with that observed for the closely related toluene analogue $Ru_2Os_3(CO)_{12}(\mu\text{-CO})(\eta^6\text{-}C_6H_5Me)$ (**5a**) [9], and is also in line with previous reports on trigonal bipyramidal pentanuclear osmium and ruthenium clusters containing arene or cyclopentadienyl ligands; without exception, the aromatic ligand always occupies an equatorial position on the pentanuclear metal framework. It has been suggested that having the $M(\eta^5\text{-}C_5H_5)$ fragment in the equatorial position enhanced the electron density donation from the equatorial to the axial sites, thereby stabilizing the cluster [5].

The crystal structure of **5** exhibited disorder, which was modelled as a disorder of one of the ruthenium atoms over two sites – M(3) and M(4). The ruthenium occupancies refined to about 0.22 and 0.78, respectively. This disorder model corresponds to two different isomers and is consistent with the solution-state ^{1}H NMR spectrum. Two identical sets of signals appear in the organic region of the ^{1}H NMR spectrum for **5** in a 3:1 integration ratio. Assignment of the spectral features for the isomers was aided by 2D NOESY and COSY experiments, and the coupling constants have also been elucidated via selective decoupling experiments. The proposed solution-state structures and tentative NMR assignments for the two isomers are shown in Fig. 5.

We have carried out a number of experiments to understand the inter-relationship among **3**–**5**; the results are summarised in Scheme 1. Cluster **5** is thermally stable and does not fragment under prolonged heating. It is thus the thermodynamic sink. It was postulated that **3** may be the precursor to **4** since these two clusters differed by two carbonyl groups. However, thermolysis of **3** only resulted in fragmentation of the cluster. On the other hand, the yields of **3** and **5** from the reaction of **1** with indene were dependent on the reaction time; prolonged thermolysis resulted in an increase in the proportion of **5** with respect to **1**. The formation of **5** must involve fragmentation of **3**. Cluster **5** was also obtainable from the co-thermolysis of **1** and **3** in cyclohexane; in the absence of **1** no conversion of **3** to **5** takes place. These results also account for the low yield of **4**. Under thermal activation, fragmentation of **3** is apparently favoured over decarbonylation to form **4**, and the resultant $Ru(\eta^5\text{-}C_9H_7)$ fragment combines with **1** to afford **5**. This presumably occurs via a pathway previously proposed for **5a**, [9] which would involve the capping of the $Ru(\eta^5\text{-}C_9H_7)$ fragment onto an $RuOs_2$ face in **1** and subsequent polyhedral

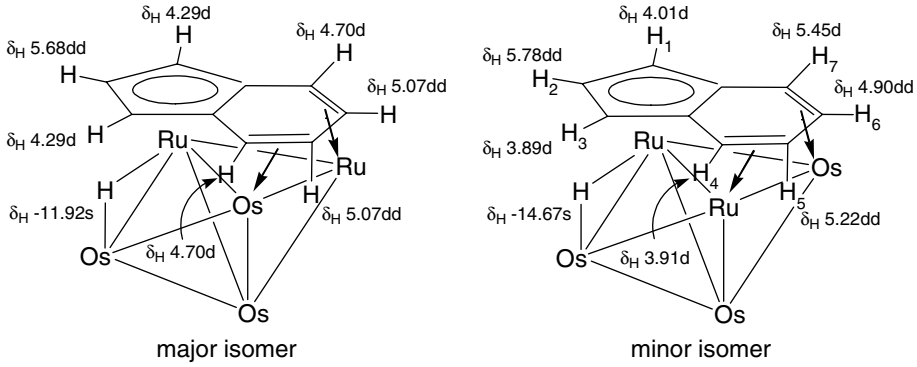

Fig. 5. Proposed solution state structures and tentative NMR assignments for **5** (carbonyls omitted). The following assignments for the minor isomer are ambiguous: H1 with H3; H4,H5 with H7,H6, respectively.

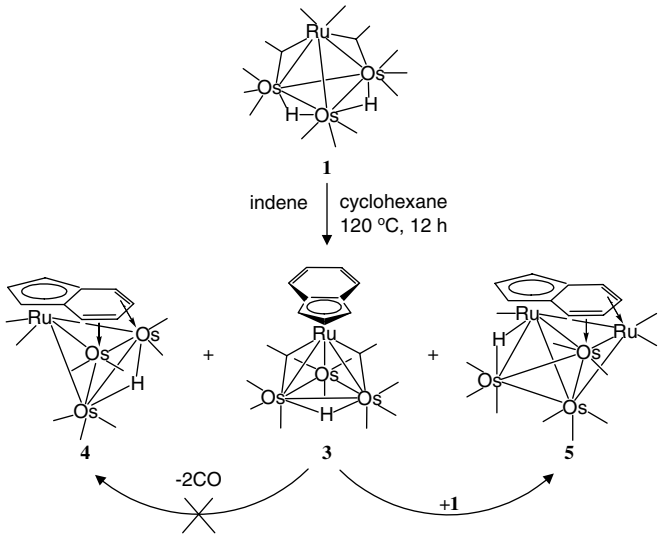

Scheme 1.

rearrangement, via a Berry pseudo-rotation, to place the fragment in an equatorial position, followed by decarbonylation and bonding of the six-membered ring of the indenyl moiety to the pentanuclear cluster [5].

3. Concluding remarks

We have thus shown that cluster **1** reacts readily with indene, initially to form **3**. The latter subsequently fragments to afford an Ru(η^5-C_9H_7) fragment which can then undergo capping reaction with **1** to give **5**, which exists as mixture of two non-interconverting isomers in solution. Decarbonylation of **3** to form **4** appears not to be favoured. Clusters **4** and **5** exhibit the novel $\mu_3,\eta^5{:}\eta^2{:}\eta^2$ bonding mode for the indenyl moiety.

4. Experimental

4.1. General procedures

All reactions and manipulations were carried out under nitrogen by using standard Schlenk techniques. Solvents were purified, dried, distilled, and stored under nitrogen prior to use. Routine NMR spectra were acquired on a Bruker ACF300 NMR spectrometer. Selective decoupling experiments and 2D NMR spectra were acquired on a Bruker Advance DRX500 or Bruker AMX500 machine. The solvent used was deuterated chloroform unless otherwise stated. Chemical shifts reported are referenced to that for the residual proton of the solvent for ^{1}H. Mass spectra were obtained on a Finnigan MAT95XL-T spectrometer in an *m*-nitrobenzyl alcohol matrix. Microanalyses were carried out by the microanalytical laboratory at the National University of Singapore. The preparation of cluster **1** appears in our earlier report [10]. All other reagents were from commercial sources and used as supplied.

4.2. Reaction of *1* with indene

To a Carius tube containing **1** (22.6 mg, 0.022 mmol) and cyclohexane (30 mL) was added indene (0.5 mL). The reaction mixture was degassed by three freeze–pump–thaw cycles, and stirred at 120 °C for 12 h. Solvent was removed under reduced pressure, and the residue so obtained was redissolved in the minimum volume of dichloromethane and chromatographed on TLC plates. Elution with hexane/dichloromethane (7:3, v/v) yielded four bands. The first and second bands were identified from their infrared spectra as **2** (1.7 mg) and unreacted **1** (3.4 mg), respectively.

Band 3 ($R_f = 0.44$) afforded dark brown crystals of **3**. Yield = 7.1 mg, 35%. IR (CH_2Cl_2) ν(CO): 2088 m, 2062 ms, 2033 s, 2005 m, 1950 w(br), 1835 w(br) cm^{-1}. ^{1}H NMR (300 K): δ 7.52 (d, 2H, $^3J_{HH} = 2.6$ Hz), 7.30 (d, 2H, $^3J_{HH} = 2.6$ Hz), 5.49 (d, 2H, $^3J_{HH} = 2.5$ Hz), 4.23 (dd, 1H, $^3J_{HH} = 2.5$ Hz), −21.66 (s, br, 1H, Os*H*Os). MS (FAB): *m*/*z* 1096 (M^+), calcd for M^+: 1096. Calcd for $C_{20}H_8O_{11}Os_3Ru.0.25C_6H_{14}$: C, 23.11; H, 1.04. Found: C, 22.78; H, 0.70%. Presence of hexane in the analytical sample was verified by ^{1}H NMR spectroscopy.

Band 4 ($R_f = 0.12$) afforded a mixture of red and black crystals, which had to be separated by hand. The red crystals were identified to be **4**. Yield = 1.7 mg, 9%. IR

(CH_2Cl_2) ν(CO): 2068 s, 2022 s cm^{-1}. ^1H NMR (300 K): δ 5.67 (m, 1H), 5.17 (m, 2H), 4.83 (m, 2H), 4.17 (m, 2H), −15.48 (s, 1H, Os*H*Os). MS (FAB): m/z 1039 (M^+), calcd for M^+: 1040.

The black crystals were identified to be **5**. Yield = 5.3 mg, 24%. IR (CH_2Cl_2) ν(CO): 2077 w, 2069 w, 2030 m, 2003 s, 1975 w, 1935 vw cm^{-1}. ^1H NMR: δ 5.68 (dd, 1H, $^3J_{HH} = 3.0$ Hz, $^3J_{HH} = 3.0$ Hz), 5.07 (dd, 2H, $^3J_{HH} = 4.1$ Hz, $^3J_{HH} = 2.5$ Hz), 4.70 (dd, 2H, $^3J_{HH} = 4.1$ Hz), 4.29 (d, 2H, $^2J_{HH} = 3.0$ Hz), −11.92 (s, 1H, Ru*H*Os) [major isomer]; 5.78 (dd, 1H,$^3J_{HH} = 3.0$ Hz, $^3J_{HH} = 3.0$ Hz), 5.45 (d, 1H, $^3J_{HH} = 5.9$ Hz), 5.22 (dd, 1H, $^3J_{HH} = 5.9$ Hz, $^3J_{HH} = 5.1$ Hz), 4.90 (dd, 1H, $^3J_{HH} = 5.9$ Hz, $^3J_{HH} = 5.1$ Hz), 4.01 (d, 1H, $^3J_{HH} = 3.0$ Hz), 3.91 (d, 1H, $^3J_{HH} = 5.9$ Hz), 3.89 (d, 1H, $^2J_{HH} = 3.0$ Hz), −14.67 (s, 1H, Ru*H*Os) [minor isomer]. MS (FAB): m/z 1196 (M^+), calcd for M^+: 1197. Calcd for $C_{20}H_8O_{11}Os_3Ru_2.0.5C_6H_{14}$: C, 22.26; H, 1.21. Found: C, 22.10; H, 1.14%. Presence of hexane in the analytical sample was verified by ^1H NMR spectroscopy.

Decreasing the reaction time to 8 h resulted in the isolation of **2** (1.5 mg), **1** (8.4 mg), **3** (8.3 mg, 55%) and **5** (1.9 mg, 12%), respectively.

4.3. Thermolysis of *3*

To a Carius tube containing cyclohexane (20 mL) was added **3** (7.3 mg, 0.007 mmol). The reaction mixture was degassed by three freeze–pump–thaw cycles, and stirred at 120 °C for 6 h. Subsequent treatment as above yielded two bands which were identified as $Os_3(CO)_{12}$ (2.6 mg) and unreacted **3** (2.8 mg), respectively.

4.4. Reaction of *1* and *3*

To a Carius tube containing cyclohexane (20 mL) was added **1** (8.1 mg, 0.008 mmol) and **3** (6.4 mg, 0.006 mmol). The reaction mixture was degassed by three freeze–pump–thaw cycles, and stirred at 120 °C for 4 h. Subsequent treatment as above yielded four bands which were identified as **2** (1.5 mg), unreacted **1** (1.3 mg), unreacted **3** (2.7 mg) and **5** (2.3 mg), respectively.

4.4.1. X-ray crystal structure determinations

Crystals were mounted on quartz fibres. X-ray data were collected on a Bruker AXS APEX system, using Mo Kα radiation, at 223 K with the SMART suite of programs [11]. Data were processed and corrected for Lorentz and polarisation effects with SAINT [12], and for absorption effects with SADABS [13]. Structural solution and refinement were carried out with the SHELXTL suite of programs [14]. Crystal and refinement data are summarised in Table 1.

The structures were solved by direct methods to locate the heavy atoms, followed by difference maps for the light, non-hydrogen atoms. The hydrides in **3** and **4** were located via low angle difference maps; they were refined freely, except that the hydride for **4** was given a fixed isotropic thermal parameter. The hydrides for **5** were placed by potential energy calculations with the program XHYDEX [15], given fixed isotropic thermal parameters, and refined riding on the osmium atom to which they we both attached. Organic hydrogen atoms were placed in calculated positions and refined with a riding model. All non-hydrogen atoms were generally given anisotropic displacement parameters in the final model. Cluster **5** exhibited disorder of the heavy atom

Table 1
Crystal and refinement data for **3**–**5**

Identification code	**3**	**4**	**5**
Empirical formula	$C_{20}H_8O_{11}Os_3Ru$	$C_{18}H_8O_9Os_3Ru$	$C_{20}H_8O_{11}Os_3Ru_2$
Formula weight	1095.93	1039.91	1197.00
Crystal system	Monoclinic	Monoclinic	Monoclinic
Space group	$P2_1/c$	$P2_1/c$	$P2_1/c$
a (Å)	8.7050(2)	9.968(4)	14.1415(5)
b (Å)	14.5480(3)	15.047(6)	9.3128(3)
c (Å)	8.9654(2)	13.743(5)	17.2702(6)
β (°)	91.0210(10)	96.688(7)	95.5620(10)
Volume (Å^3)	1135.20(4)	2047.2(13)	2263.72(13)
Z	2	4	4
ρ_c (Mg/m^3)	3.206	3.374	3.512
μ (mm^{-1})	17.448	19.333	18.142
F(000)	976	1840	2128
Crystal size (mm^3)	0.38 × 0.24 × 0.16	0.19 × 0.12 × 0.10	0.12 × 0.08 × 0.06
Theta range for data collection, deg	2.27 to 30.51	2.01 to 26.37	2.37 to 26.37
Reflections collected	10492	28437	31158
Independent reflections [R(int)]	3410 [0.0314]	4187 [0.0405]	4635 [0.0383]
Maximum and minimum transmission	0.1667 and 0.0578	0.2480 and 0.1203	0.4090 and 0.2194
Data/restraints/parameters	3410/0/169	41877/0/283	4635/3/332
Goodness-of-fit on F^2	1.106	1.067	1.089
Final R indices [$I > 2\sigma(I)$]	$R_1 = 0.0272$, $wR_2 = 0.0650$	$R_1 = 0.0271$, $wR_2 = 0.0615$	$R_1 = 0.0354$, $wR_2 = 0.0897$
R indices (all data)	$R_1 = 0.0305$, $wR_2 = 0.0662$	$R_1 = 0.0335$, $wR_2 = 0.0639$	$R_1 = 0.0388$, $wR_2 = 0.0914$
Largest difference in peak and hole, e Å^{-3}	1.343 and −2.503	2.816 and −1.023	2.472 and −3.338

positions; one of the ruthenium atoms was modelled as disordered over two sites, M(3) and M(4), and the Ru occupancies were refined to about 0.22 and 0.78, respectively.

5. Supplementary material

Crystallographic data (excluding structure factors) for the structures in this paper have been deposited with the Cambridge Crystallographic Data Centre. CCDC 620444, 620445 and 620446 contain the supplementary crystallographic data for this paper. These data can be obtained free of charge via http://www.ccdc.cam.ac.uk/conts/retrieving.html, or from the Cambridge Crystallographic Data Centre, 12 Union Road, Cambridge CB2 1EZ, UK; fax: (+44) 1223-336-033; or e-mail: deposit@ccdc.cam.ac.uk.

Acknowledgements

This work was supported by the National University of Singapore (Research Grant No. R143-000-267-112) and one of us (Y.L.K.T.) thanks the University for a Research Scholarship.

References

[1] G.M. Diamond, M.L.H. Green, P. Mountford, N.A. Popham, A.N.J. Chernaga, Chem. Soc., Chem. Commun. (1994) 103.
[2] (a) A. Eisenstadt, F. Frolow, A. Efraty, J. Chem. Soc., Chem. Commun. (1982) 642;
(b) H. Chen, B.F.G. Johnson, J. Lewis, P.R. Raithby, J. Chem. Soc., Chem. Commun. (1990) 373;
(c) H. Chen, M. Fajardo, B.F.G. Johnson, J. Lewis, P.R. Raithby, J. Organomet. Chem. 389 (1990) C16;
(d) A.J. Arce, Y. De Santis, R. Machado, J. Manzur, M.V. Capparelli, Organometallics 15 (1996) 1834;
(e) H. Nagashima, A. Suzuki, H. Kondo, M. Nobata, K. Aoki, K. Itoh, J. Organomet. Chem. 580 (1999) 239;
(f) P. Schooler, B.F.G. Johnson, L. Scaccianoce, J. Danheim, H. Hopf, J. Chem. Soc., Dalton Trans. (2000) 199.
[3] D. Chen, B. Mu, S. Xu, B. Wang, J. Organomet. Chem. 691 (2006) 3823.
[4] R. Buntem, J. Lewis, C.A. Morewood, P.R. Raithby, M.C.R. de Arellano, G.P. Shields, J. Chem. Soc., Dalton Trans. (1998) 1091.
[5] P.R. Raithby, G.P. Shields, Polyhedron 17 (1998) 2829.
[6] (a) J.R. Fox, W.L. Gladfelter, T.G. Wood, J.A. Smegal, T.K. Foreman, G.L. Geoffroy, I. Tavanaipour, V.W. Day, C.S. Day, Inorg. Chem. 20 (1981) 3214;
(b) W.L. Gladfelter, G.L. Geoffroy, Inorg. Chem. 19 (1980) 2579.
[7] J. Lewis, P.R. Raithby, G.N. Ward, J. Chem. Soc., Chem. Commun. (1995) 755.
[8] R.K. Pomeroy, in: G. Wilkinson, F.G.A. Stone, E.W. Abel (Eds.), Comprehensive Organometallic Chemistry II, vol. 7, Pergamon Press, 1995, chapter 15.
[9] Y.L.K. Tan, W.K.J. Leong, Organomet. Chem. 691 (2006) 2048.
[10] L. Pereira, W.K. Leong, S.Y.J. Wong, Organomet. Chem. 609 (2000) 104.
[11] SMART version 5.628, Bruker AXS Inc., Madison, Wisconsin, USA, 2001.
[12] SAINT+ version 6.22a, Bruker AXS Inc., Madison, Wisconsin, USA, 2001.
[13] G.M. Sheldrick, SADABS, 1996.
[14] SHELXTL version 5.1, Bruker AXS Inc., Madison, Wisconsin, USA, 1997.
[15] A.G. Orpen, XHYDEX, School of Chemistry, University of Bristol, UK, 1997.